

Review

Status of the SACLA Facility

Makina Yabashi ^{1,*}, Hitoshi Tanaka ¹, Kensuke Tono ² and Tetsuya Ishikawa ¹

¹ RIKEN SPring-8 Center, 1-1-1 Kouto, Sayo-cho, Sayo-gun, Hyogo 679-5148, Japan; tanaka@spring8.or.jp (H.T.); ishikawa@spring8.or.jp (T.I.)

² Japan Synchrotron Radiation Research Institute, 1-1-1 Kouto, Sayo-cho, Sayo-gun, Hyogo 679-5198, Japan; tonos@spring8.or.jp

* Correspondence: yabashi@spring8.or.jp; Tel.: +81-791-58-0802

Academic Editor: Kiyoshi Ueda

Received: 12 May 2017; Accepted: 8 June 2017; Published: 10 June 2017

Abstract: This article reports the current status of SACLA, SPring-8 Angstrom Compact free electron LAsER, which has been producing stable X-ray Free Electron Laser (XFEL) light since 2012. A unique injector system and a short-period in-vacuum undulator enable the generation of ultra-short coherent X-ray pulses with a wavelength shorter than 0.1 nm. Continuous development of accelerator technologies has steadily improved XFEL performance, not only for normal operations but also for fast switching operation of the two beamlines. After upgrading the broadband spontaneous-radiation beamline to produce soft X-ray FEL with a dedicated electron beam driver, it is now possible to operate three FEL beamlines simultaneously. Beamline/end-station instruments and data acquisition/analyzation systems have also been upgraded to allow advanced experiments. These efforts have led to the production of novel results and will offer exciting new opportunities for users from many fields of science.

Keywords: X-ray free electron laser; SACLA; linac; undulator; X-ray optics; photon diagnostics; damage-free analysis; ultrafast science

1. Introduction

SACLA, SPring-8 Angstrom Compact free electron LAsER, is an X-ray Free Electron Laser (XFEL) facility at SPring-8, Japan. It was inaugurated in March 2012 [1], becoming the second XFEL facility in the world, following the 2009 inauguration of LCLS, the Linac Coherent Light Source, at SLAC in the US [2]. The LCLS and the European XFEL [3] at DESY in Germany, which were first proposed in the 1990s, utilize high-energy linacs with beam energies around 15 GeV and lengths of a few kilometers to produce short wavelength XFEL radiation. In contrast, SACLA was designed as the first compact XFEL facility to produce brilliant and stable XFEL radiation with substantially lower costs for construction and operations. To enable this, we employed unique accelerator technologies: a low emittance injector with a thermionic electron gun (e-gun) and a velocity bunching system; a high-gradient normal-conducting C-band linac; and a short-period in-vacuum undulator [4]. Combining these devices with state-of-the-art X-ray optics [5,6], we have steadily generated XFEL light for users more than 4000 h in FY2016, allowing researchers to produce a number of important scientific results in the fields of biology [7–12], chemistry [13–16], materials science [17–20], high-energy density science [21], and non-linear X-ray optics [22–26]. The success of SACLA has promoted the development of similar compact XFEL facilities, such as SwissFEL at Paul Scherrer Institut in Switzerland [27].

In parallel to conducting user operations, we have continued to upgrade the facility. One of the most critical demands from users is to increase beam time, which recently led us to construct new beamlines and to develop an innovative scheme to switch XFEL over multiple beamlines in a pulse-by-pulse manner [28]. We have also developed various new beamline/end-station instruments and data acquisition/analysis systems to advance experimental capabilities [29–37].

Over the years, we have published several articles about the SACLA facility. In [1], we reported the concept, design, and initial performance of SACLA. Tono et al. also reported the initial beamline design and performance [5]. In [6], we provided updated information on beam performance, beamline instruments, and early scientific highlights. In this article, we report the current status of SACLA, including recent scientific achievements and new capabilities enabled in early 2017. In Section 2, we summarize the typical performance of a hard X-ray FEL beamline, BL3, with the updated design. Section 3 describes recent scientific highlights and the advanced technologies that enable these achievements. In Section 4, we review the construction and operation of two new beamlines, BL2 and BL1. Finally, Section 5 presents our plans for the future.

2. Typical Performance

Table 1 shows basic radiation characteristics for the first XFEL beamline, BL3. The unique injector system combines an e-gun using a thermionic cathode and a multi-stage bunch compression system, instead of an RF-photo cathode system. This configuration can produce high peak power with an X-ray pulse duration shorter than 10 fs under normal operating conditions. Such a short pulse duration assures analysis with a “diffraction-before-destruction” scheme and potentially facilitate ultrafast experiments.

Table 1. Typical characteristics for the X-ray Free Electron Laser (XFEL) light of beamline 3 (BL3).

Parameter	Typical Value
Pulse energy	~0.5 mJ at 10 keV
Pulse duration	<10 fs
Peak power	>50 GW
Photon energy (Wavelength)	4.0–20 keV ¹ (0.062–0.31 nm)
Bandwidth	0.5% (FWHM ²)
Repetition rate	60 Hz maximum

¹ 4.0–15 keV in daily operation. ² Full width at half maximum.

The beamline provides hard X-ray FEL with a high photon energy, greater than ~15 keV, even with a moderate beam energy of 8 GeV. This distinct capability is possible due to the in-vacuum short-period undulator, a core device adopted for our compact XFEL machine. Furthermore, shorter wavelength X-rays can be produced while fixing the electron beam energy by decreasing the magnetic field by opening a gap between the undulator magnets. This variable-gap design enables the production of two-color XFEL pulses with a wavelength separation above 30% using a simple split undulator technique, where the undulator gaps between the upstream and downstream sections are changed [38].

In the autumn of 2016, the first user experiment to use the maximum repetition rate of 60 Hz took place. The standard repetition rate in daily operations has increased steadily and will be 60 Hz during the latter half of 2017. Figure 1 shows a typical trend graph of pulse energy for user experiments. The constant output with a small fluctuation of 16% in root mean square (rms) demonstrates the high stability of operations, another important feature of SACLA operations. The mean fault interval in 2016 was more than 1 h at a repetition rate of 30 Hz.

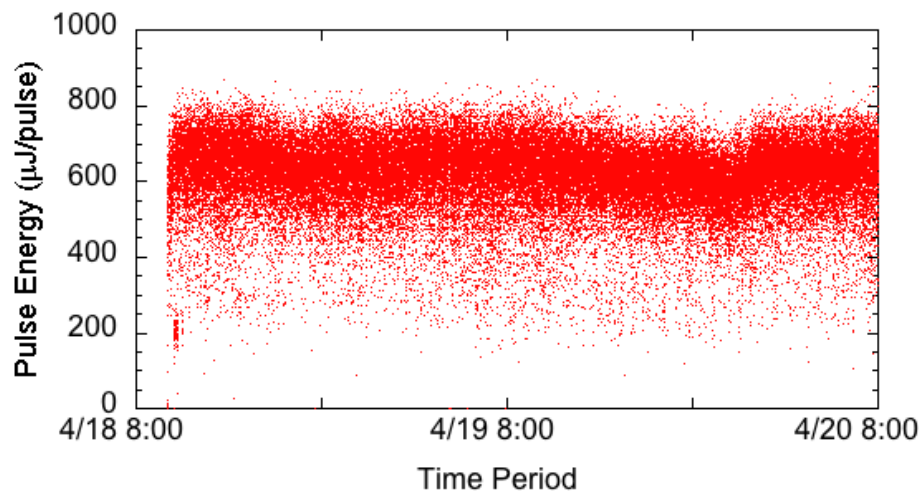


Figure 1. Trend of XFEL (X-ray Free Electron Laser) pulse energy at BL3 over 48 h on 18–20 April 2016. The average and peak pulse energies were 0.61 mJ and 0.87 mJ, respectively, at a photon energy of 10 keV. The rms pulse-energy fluctuation was 16%.

Figure 2 shows the current schema for BL3. In the original design, the beamline had only basic functions, such as beam transport, monochromatization, focusing, and monitoring of fundamental beam parameters [5]. The beam-transport optical system basically consists of two sets of double plane mirrors and a double crystal monochromator (DCM). One of the mirror sets or DCM is selected to deliver a beam that is pink or monochromatic, respectively. The double mirror systems with different glancing angles (2 and 4 mrad) reflect X-rays below cutoff energies and attenuates the higher order harmonics above them. The DCM with Si (111) crystals delivers a monochromatic beam with a bandwidth of $\sim 10^{-4}$ ($\Delta E/E$). The standard focusing optical device is a Kirkpatrick–Baez mirror pair, which is stationed at an experimental hutch to provide a 1 μm X-ray spot [30]. In the upgraded beamline, new functions have been added to support broader and more advanced applications. The following major upgrades have been applied:

Beam-transport and 1 μm focusing mirrors were replaced with longer ones to increase acceptable beam sizes, especially in the lower photon energy ranges with a larger beam size [39]. Transmission ratios from the source to the sample position were improved from 30% to 55% at 5.5 keV, from 46% to 61% at 7.0 keV, and from 59% to 65% at 10 keV.

- Transmission gratings working as beam splitters were installed in an optics hutch (OH2). The gratings are used for simultaneous diagnostics of timing [36] and/or spectrum [29] at the first experimental hutch EH1 with user experiments performed at another experimental hutch [37].
- A diamond phase retarder was stationed in OH2 for the polarization control of XFEL light [40].
- Compound refractive lenses made of beryllium were installed in EH2.
- A two-stage focusing system was deployed at EH4c and EH5 to produce a 50 nm X-ray spot [32].

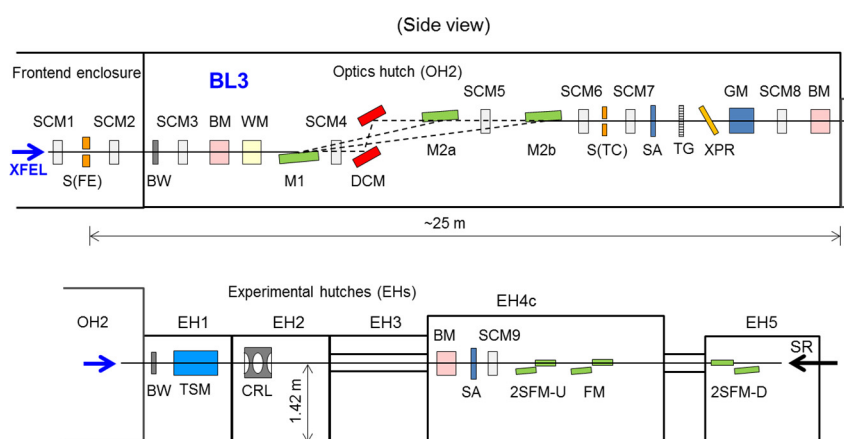


Figure 2. Major optical and diagnostic systems of SACLA BL3. SCM: screen monitor; S(FE): frontend slit; BW: beryllium window; BM: beam intensity and position monitor; WM: wavelength monitor; M1, M2a, M2b: plane mirrors; DCM: double crystal monochromator; S(TC): transport-channel slit; SA: solid attenuator; TG: transmission grating; XPR: X-ray phase retarder; GM: gas intensity monitor; TSM: timing and spectrum monitor; CRL: compound refractive lens; 2SFM-U(-D): two-stage focusing mirrors on the upstream (downstream) side (50 nm spot size); FM: focusing mirrors (1 μm spot size); SR: synchrotron radiation from SPring-8.

A more detailed description of the new components/functions will be provided in a separate article [41]. These state-of-the-art X-ray optics and diagnostics enable advanced experiments, such as X-ray nonlinear optics under ultrahigh intensity over 10^{20} W/cm^2 , achieved with the two-stage focusing system.

3. Recent Scientific Highlights and New Instruments

To enable a deeper understanding of the photosynthetic process so that we can design artificial photosynthesis, it is important to determine the structures and functions of photosystem II (PSII), a key catalytic protein complex for photosynthesis. Shen and team achieved a milestone by determining the “radiation-damage-free” structure of PSII in the S_1 state at a resolution of 1.95 \AA with SACLA. Their results show differences at the sub-angstrom level, compared to those obtained with a quasi-CW X-ray source of synchrotron radiation [10]. Furthermore, they determined the structure of an intermediate S_3 state with two-flash illumination at room temperature at a resolution of 2.35 \AA with a time-resolved (TR) serial femtosecond crystallography (SFX) method. This finding suggests the insertion of a new oxygen atom close to an existing oxygen atom in the molecule [11]. These results provide a critical basis for understanding the mechanisms underlying oxygen evolution in photosynthesis.

The TR-SFX method was also used to determine conformational changes in bacteriorhodopsin (bR), a light-driven proton pump, and a model membrane transport protein, at 13 time points in a scale ranging from nanoseconds to milliseconds following photo activation [12]. The resulting molecular movie elucidated a fundamental mechanism for directional proton transport in bR.

These achievements were supported by an experimental platform named DAPHNIS developed by the SACLA team [34]. This instrument is composed of a small He chamber for sample injection and a short-work-distance MPCCD detector with octal sensors that is separated from the chamber [31]. This design offers great flexibility to efficiently meet various demands from users, including introduction of new types of sample injectors, such as grease-matrix and droplet injectors [9,42], and extensions to pump-probe experiments.

The pump-probe scheme was applied for X-ray analysis based on wide-angle scattering (WAXS) of solution. Ihee and Adachi et al. observed a formation process for a gold complex $[\text{Au}(\text{CN})_2]_3$ in solution after excitation of an ultrafast laser pulse with a wavelength of 267 nm [14]. The time

resolution in this experiment was sub-picosecond, limited mainly by arrival timing jitter between the XFEL and optical laser pulses.

To improve the time resolution, we developed an arrival timing monitor by probing the ultrafast change in optical transmittance induced by intense XFEL light with a spatial decoding technique [36,37]. A unique feature of our optical design is the utilization of an X-ray elliptical mirror for increasing X-ray intensity to form a line-focused profile, which suppresses the X-ray pulse energy that is required to be as small as several microjoules at ~10 keV. Furthermore, we developed a beam branching system for enabling timing diagnostics to be determined simultaneously with experiments. The system is based on a transmission grating that creates two branches dedicated for timing and spectral diagnostics in addition to the 0th order branch used for the main experiments [43]. We evaluated the accuracy of the monitor by constructing a similar setup in the main branch and found that the error was as small as 7 fs in rms. We compared our system with another timing monitor based on the THz streaking method constructed by the PSI group, which assured a relative accuracy of 16.7 fs [44]. This system is now routinely used for pump-probe experiments and contributes to improving time resolution down to a few tens of fs.

The two-color generation configuration based on the split-undulator technique can be combined with the two-stage tight X-ray focusing system, enabling researchers to investigate the non-linear interactions between intense X-ray fields and matter [32,38]. The generation of a Cu K α laser marked a significant achievement. The Cu target was excited with ultra-intense 9-keV X-rays to produce K-shell vacancies and to form the population inversion condition, leading to the generation of amplified spontaneous emission on Cu K α lines [26]. Furthermore, while operating SACLA in the two-color mode, we observed the efficient amplification of 8 keV X-rays induced as a seeding.

In this two-color mode, the temporal separation of two XFEL pulses could be tuned with a sub-fs resolution by using a small chicane of the electron beam in the middle of the undulator line. In the summer of 2016, the maximum separation of 40 fs for the 8 GeV electron beam was extended to ~300 fs by increasing the maximum current for the chicane magnets. Based on this scheme, an X-ray pump and X-ray probe experiment was performed to investigate the fundamental damage processes in a diamond induced by intense 6.1 keV X-rays [45]. It was found that the diffraction signal of the 5.9 keV probe pulse decreased after 20 fs following pump pulse irradiation with an intensity of 10^{19} W/cm 2 due to the X-ray-induced atomic displacement. This finding offers a valuable opportunity for experimental evaluation of the “diffraction-before-destruction” scheme.

We developed a hard X-ray split-and-delay optical (SDO) system based on the Bragg diffraction in crystal optics for generating two split pulses with a variable temporal separation [46–48]. To achieve both high stability and operational flexibility, the SDO system was designed to include both variable-delay and fixed-delay branches. As key optical elements, we fabricated high-quality thin crystals and channel-cut crystals by applying the plasma chemical vaporization machining technique. The SDO system using Si(220) crystals covered a photon energy range of 6.5–11.5 keV and a delay time range from a negative value to >45 ps over the photon energy range (up to 220 ps at 6.5 keV). We developed a simple alignment method for achieving a spatial overlap between the split pulses. This SDO system was tested at BL29XU of SPring-8 in combination with a focusing system. We achieved an excellent overlap with an accuracy of 30 nm for ~200 nm focused beams in both the horizontal and vertical directions. This result marks a milestone towards the realization of time-resolved studies using multiple X-ray pulses with a time range from femtosecond to sub-nanosecond scales at XFEL facilities.

4. New Beamlines

Figure 3 shows the schematic view of the current SACLA facility with three beamlines. In 2015, we constructed a second hard X-ray FEL beamline, BL2, and tested pulse-to-pulse switching operations between BL2 and BL3, the first hard XFEL beamline, by using a fast kicker magnet in the upstream location of the undulator lines [28]. At that time, we found that the quality of an electron beam was degraded at a dog-leg transport with a deflection angle of ± 3 degrees to the BL2 undulators.

The highly compressed electron beam with a peak current greater than 10 kA produced unwanted coherent synchrotron radiation (CSR), which significantly enlarged the electron beam emittance through large energy modulation in the dipole magnets. To resolve this issue, we redesigned the optics of the dog-leg transport to include a combination of two double-bend achromat structures while maintaining high symmetry. Furthermore, we developed a pulsed high power supply to increase the deflection angle of the switching magnet. In February 2017, we tested this system and found that high pulse energies of several hundred microjoules were simultaneously generated at the two beamlines by employing the highly compressed electron beam. Later in 2017, we plan to offer simultaneous operations of these beamlines for users.

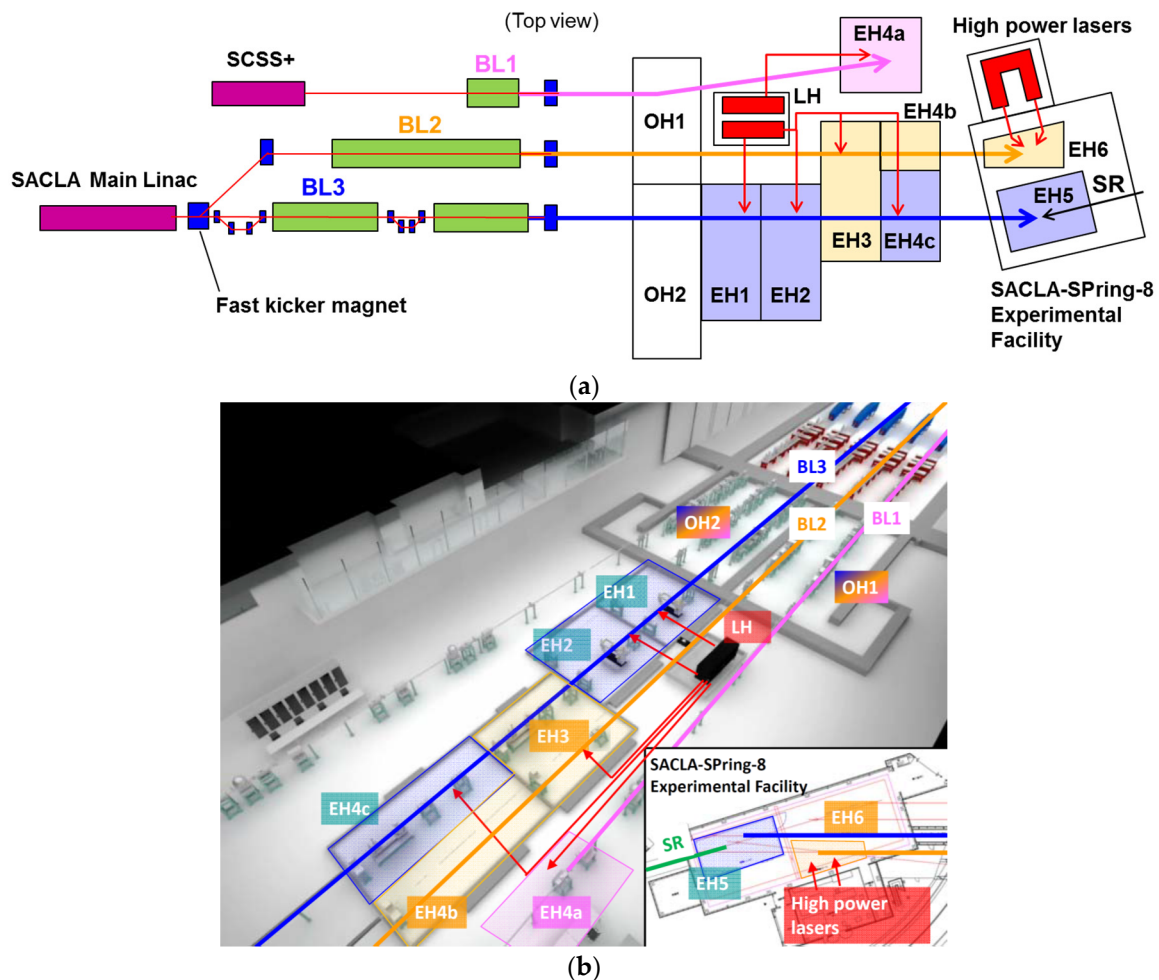


Figure 3. (a) Schematic top view of the SACLA facility. Purple bars in (a) indicate linacs and green bars indicate undulators. OH: optics hutch; EH: experimental hutch; LH: laser hutch; SR: synchrotron radiation from SPring-8. (b) Schematic bird's eye view of the SACLA experimental hall.

In 2015, we also upgraded the broadband spontaneous radiation beamline BL1 to a soft X-ray FEL beamline. A key machine used for this project was the SPring-8 Compact SASE Source (SCSS) test accelerator [4]. This machine was built in 2005 with a beam energy of 250 MeV, originally for performing proof-of-principle tests for the compact XFEL scheme. Following the first lasing at 49 nm in 2006, SCSS was also used for R&D on FEL utilization and experiments with intense FEL radiation in the extreme ultraviolet (EUV) region. In 2013, SCSS was decommissioned after the successful inauguration of SACLA. However, we found space in the upstream position of the BL1 undulator to accommodate this machine as a compact electron beam driver dedicated to BL1. In the summer of 2015, we relocated the accelerator components of SCSS while increasing the beam energy to 450 MeV. This upgraded

machine is called SCSS+. In October 2015, we achieved first lasing at a photon energy of 37 eV, and started user operations the following July. In the summer of 2016, we further added two accelerator units to increase the beam energy to 800 MeV. We observed a high pulse energy above 100 μJ at a photon energy around 100 eV before the winter shutdown of 2016. The typical energy resolution is $\sim 2\%$. Since we use an in-vacuum variable-gap undulator for BL1, i.e., the same as that used for BL2 and BL3, we can cover a higher photon energy up to ~ 150 eV by opening the undulator gap while maintaining pulse energy above ~ 10 μJ . It should be emphasized that SCSS+ and SACLA are operated independently, so we are able to increase the available user time of soft X-ray FEL without limiting the availability of hard X-ray FEL at BL2 and BL3.

5. Plans for the Future

We continue to upgrade SACLA not only to enhance the performance and availability of XFEL but also to establish a technological foundation for the future SPring-8-II, our upgrade of the existing SPring-8 facility. The unique capability to operate multiple FEL beamlines allows us to offer exciting research opportunities with new experimental schemes. For example, BL1 and BL2/BL3 can be synchronized to provide FEL pulses with a finely controlled time interval because both the SCSS+ and SACLA linacs use a common trigger source. This synchronized operation will enable pump and probe experiments with both soft and hard X-ray FELs.

Pulse-by-pulse switching is presently realized in a scheme that distributes laser pulses equally over multiple beamlines. In this scheme, an equivalent number of pulses is delivered to each beamline. However, depending on the combination of experiments at BL2 and BL3, one beamline may require more pulses than the other. A flexible control system enabling an arbitrary pulse distribution, e.g., 40 pulses/s at BL2 and 20 at BL3, is under development to improve the utilization efficiency.

On the other hand, we plan to use the SACLA linac as an injector for SPring-8-II. Although the dynamic aperture of SPring-8-II is much narrower than the current one, the small emittance beams from the SACLA linac can maintain excellent injection efficiency with high stability. Another advantage of this scheme is that we can save massive amounts of electricity by stopping operations of the existing SPring-8 injector composed of the 8 GeV booster synchrotron and 1 GeV linac. However, this scenario of sharing the SACLA linac between SACLA and SPring-8-II requires two major developments: one is to change the bunch length in a pulse-by-pulse manner to keep the small beam emittance at the injection point of the ring; the other is to enable “on-demand beam injection” that accepts injection requests from the ring for the top-up operation. The first test of beam injection from the SACLA linac to the current storage ring is scheduled for FY2018.

Acknowledgments: The authors are grateful to all of the SACLA/SPring-8 staff who have participated in the construction and operation of SACLA.

Author Contributions: All authors wrote the paper on behalf of the SACLA team.

Conflicts of Interest: The authors declare no conflict of interest.

References

1. Ishikawa, T.; Aoyagi, H.; Asaka, T.; Asano, Y.; Azumi, N.; Bizen, T.; Ego, H.; Fukami, K.; Fukui, T.; Furukawa, Y.; et al. A compact X-ray free-electron laser emitting in the sub-ångstrom region. *Nat. Photonics* **2012**, *6*, 540–544. [[CrossRef](#)]
2. Emma, P.; Akre, R.; Arthur, J.; Bionta, R.; Bostedt, C.; Bozek, J.; Brachmann, A.; Bucksbaum, P.; Coffee, R.; Decker, F.-J.; et al. First lasing and operation of an ångstrom-wavelength free-electron laser. *Nat. Photonics* **2010**, *4*, 641–647. [[CrossRef](#)]
3. Altarelli, M. The European X-ray Free-Electron Laser Facility in Hamburg. *Nucl. Instrum. Methods B* **2011**, *269*, 2845–2849. [[CrossRef](#)]

4. Shintake, T.; Tanaka, H.; Hara, T.; Tanaka, T.; Togawa, K.; Yabashi, M.; Otake, Y.; Asano, Y.; Bizen, T.; Fukui, T.; et al. A compact free-electron laser for generating coherent radiation in the extreme ultraviolet region. *Nat. Photonics* **2008**, *2*, 555–559. [[CrossRef](#)]
5. Tono, K.; Togashi, T.; Inubushi, Y.; Sato, T.; Katayama, T.; Ogawa, K.; Ohashi, H.; Kimura, H.; Takahashi, S.; Takeshita, K.; et al. Beamline, experimental stations and photon beam diagnostics for the hard X-ray free electron laser of SACLA. *New J. Phys.* **2013**, *15*, 083035. [[CrossRef](#)]
6. Yabashi, M.; Tanaka, H.; Ishikawa, T. Overview of the SACLA facility. *J. Synchrotron Rad.* **2015**, *22*, 477–484. [[CrossRef](#)] [[PubMed](#)]
7. Kimura, T.; Joti, Y.; Shibuya, A.; Song, C.; Kim, S.; Tono, K.; Yabashi, M.; Tamakoshi, M.; Moriya, T.; Oshima, T.; et al. Imaging live cell in micro-liquid enclosure by X-ray laser diffraction. *Nat. Commun.* **2014**, *5*, 3052. [[CrossRef](#)] [[PubMed](#)]
8. Hirata, K.; Shinzawa-Itoh, K.; Yano, N.; Takemura, S.; Kato, K.; Hatanaka, M.; Muramoto, K.; Kawahara, T.; Tsukihara, T.; Yamashita, E.; et al. Determination of damage-free crystal structure of an X-ray-sensitive protein using an XFEL. *Nat. Methods* **2014**, *11*, 734–736. [[CrossRef](#)] [[PubMed](#)]
9. Sugahara, M.; Mizohata, E.; Nango, E.; Suzuki, M.; Tanaka, T.; Masuda, T.; Tanaka, R.; Shimamura, T.; Tanaka, Y.; Suno, C.; et al. Grease matrix as a versatile carrier of proteins for serial crystallography. *Nat. Methods* **2015**, *12*, 61–63. [[CrossRef](#)] [[PubMed](#)]
10. Suga, M.; Akita, F.; Hirata, K.; Ueno, G.; Murakami, H.; Nakajima, Y.; Shimizu, T.; Yamashita, K.; Yamamoto, M.; Ago, H.; Shen, J.-R. Native structure of photosystem II at 1.95 Å resolution viewed by femtosecond X-ray pulses. *Nature* **2015**, *517*, 99–103. [[CrossRef](#)] [[PubMed](#)]
11. Suga, M.; Akita, F.; Sugahara, M.; Kubo, M.; Nakajima, Y.; Nakane, T.; Yamashita, K.; Umena, Y.; Nakabayashi, M.; Yamane, T.; et al. Light-induced structural changes and the site of O=O bond formation in PSII caught by XFEL. *Nature* **2017**, *543*, 131–135. [[CrossRef](#)] [[PubMed](#)]
12. Nango, E.; Royant, A.; Kubo, M.; Nakane, T.; Wickstrand, C.; Kimura, T.; Tanaka, T.; Tono, K.; Song, C.; Tanaka, R.; et al. A three-dimensional movie of structural changes in bacteriorhodopsin. *Science* **2016**, *354*, 1552–1557. [[CrossRef](#)] [[PubMed](#)]
13. Obara, Y.; Katayama, T.; Ogi, Y.; Suzuki, T.; Kurahashi, N.; Karashima, S.; Chiba, Y.; Isokawa, Y.; Togashi, T.; Inubushi, Y.; et al. Femtosecond time-resolved X-ray absorption spectroscopy of liquid using a hard X-ray free electron laser in a dual-beam dispersive detection method. *Opt. Express* **2014**, *22*, 1105–1113. [[CrossRef](#)] [[PubMed](#)]
14. Kim, K.H.; Kim, J.G.; Nozawa, S.; Sato, T.; Oang, K.Y.; Kim, T.W.; Ki, H.; Jo, J.; Park, S.; Song, C.; et al. Direct observation of bond formation in solution with femtosecond X-ray scattering. *Nature* **2015**, *518*, 385–389. [[CrossRef](#)] [[PubMed](#)]
15. Uemura, Y.; Kido, D.; Wakisaka, Y.; Uehara, H.; Ohba, T.; Niwa, Y.; Nozawa, S.; Sato, T.; Ichianagi, K.; Fukaya, R.; et al. Dynamics of photoelectrons and structural changes of tungsten trioxide observed by femtosecond transient XAFS. *Angew. Chem. Int. Ed.* **2016**, *55*, 1364–1367. [[CrossRef](#)] [[PubMed](#)]
16. Canton, S.E.; Kjær, K.S.; Vankó, G.; van Driel, T.B.; Adachi, S.; Bordage, A.; Bressler, C.; Chabera, P.; Christensen, M.; Dohn, A.O.; et al. Visualizing the non-equilibrium dynamics of photoinduced intramolecular electron transfer with femtosecond X-ray pulses. *Nat. Commun.* **2015**, *6*, 6359. [[CrossRef](#)] [[PubMed](#)]
17. Takahashi, Y.; Suzuki, A.; Zetsu, N.; Oroguchi, T.; Takayama, Y.; Sekiguchi, Y.; Kobayashi, A.; Yamamoto, M.; Nakasako, M. Coherent diffraction imaging analysis of shape-controlled nanoparticles with focused hard X-ray free-electron laser pulses. *Nano Lett.* **2013**, *13*, 6028–6032. [[CrossRef](#)] [[PubMed](#)]
18. Mitrofanov, K.V.; Fons, P.; Makino, K.; Terashima, R.; Shimada, T.; Kolobov, A.V.; Tominaga, J.; Bragaglia, V.; Giussani, A.; Calarco, R.; et al. Sub-nanometre resolution of atomic motion during electronic excitation in phase-change materials. *Sci. Rep.* **2016**, *6*, 20633. [[CrossRef](#)] [[PubMed](#)]
19. Dean, M.P.M.; Cao, Y.; Liu, X.; Wall, S.; Zhu, D.; Mankowsky, R.; Thampy, V.; Chen, X.M.; Vale, J.G.; Casa, D.; et al. Ultrafast energy- and momentum-resolved dynamics of magnetic correlations in the photo-doped Mott insulator Sr₂IrO₄. *Nat. Mater.* **2016**, *15*, 601–605. [[CrossRef](#)] [[PubMed](#)]
20. Matsubara, E.; Okada, S.; Ichitsubo, T.; Kawaguchi, T.; Hirata, A.; Guan, P.F.; Tokuda, K.; Tanimura, K.; Matsunaga, T.; Chen, M.W.; Yamada, N. Initial atomic motion immediately following femtosecond-laser excitation in phase-change materials. *Phys. Rev. Lett.* **2016**, *117*, 135501. [[CrossRef](#)] [[PubMed](#)]

21. Hartley, N.J.; Ozaki, N.; Matsuoka, T.; Albertazzi, B.; Faenov, A.; Fujimoto, Y.; Habara, H.; Harmand, M.; Inubushi, Y.; Katayama, T.; et al. Ultrafast observation of lattice dynamics in laser-irradiated gold foils. *Appl. Phys. Lett.* **2017**, *110*, 071905. [[CrossRef](#)]
22. Fukuzawa, H.; Son, S.-K.; Motomura, K.; Mondal, S.; Nagaya, K.; Wada, S.; Liu, X.-J.; Feifel, R.; Tachibana, T.; Ito, Y.; et al. Deep inner-shell multiphoton ionization by intense X-ray free-electron laser pulses. *Phys. Rev. Lett.* **2013**, *110*, 173005. [[CrossRef](#)] [[PubMed](#)]
23. Tamasaku, K.; Shigemasa, E.; Inubushi, Y.; Katayama, T.; Sawada, K.; Yumoto, H.; Ohashi, H.; Mimura, H.; Yabashi, M.; Yamauchi, K.; Ishikawa, T. X-ray two-photon absorption competing against single and sequential multiphoton processes. *Nat. Photonics* **2014**, *8*, 313–316. [[CrossRef](#)]
24. Shwartz, S.; Fuchs, M.; Hastings, J.B.; Inubushi, Y.; Ishikawa, T.; Katayama, T.; Reis, D.A.; Sato, T.; Tono, K.; Yabashi, M.; et al. X-ray second harmonic generation. *Phys. Rev. Lett.* **2014**, *112*, 163901. [[CrossRef](#)] [[PubMed](#)]
25. Yoneda, H.; Inubushi, Y.; Yabashi, M.; Katayama, T.; Ishikawa, T.; Ohashi, H.; Yumoto, H.; Yamauchi, K.; Mimura, H.; Kitamura, H. Saturable absorption of intense hard X-rays in iron. *Nat. Commun.* **2014**, *5*, 5080. [[CrossRef](#)] [[PubMed](#)]
26. Yoneda, H.; Inubushi, Y.; Nagamine, K.; Michine, Y.; Ohashi, H.; Yumoto, H.; Yamauchi, K.; Mimura, H.; Kitamura, H.; Katayama, T.; et al. Atomic inner-shell laser at 1.5-ångström wavelength pumped by an X-ray free-electron laser. *Nature* **2015**, *524*, 446–449. [[CrossRef](#)] [[PubMed](#)]
27. Ganter, R. (Ed.) *SwissFEL Conceptual Design Report*; PSI Report 10-04; PSI: Villigen, Switzerland, 2010.
28. Hara, T.; Fukami, K.; Inagaki, T.; Kawaguchi, H.; Kinjo, R.; Kondo, C.; Otake, Y.; Tajiri, Y.; Takebe, H.; Togawa, K.; et al. Pulse-by-pulse multi-beam-line operation for X-ray free-electron lasers. *Phys. Rev. ST AB* **2016**, *19*, 020703. [[CrossRef](#)]
29. Inubushi, Y.; Tono, K.; Togashi, T.; Sato, T.; Hatsui, T.; Kameshima, T.; Togawa, K.; Hara, T.; Tanaka, T.; Tanaka, H.; et al. Determination of the pulse duration of an X-ray free electron laser using highly resolved single-shot spectra. *Phys. Rev. Lett.* **2012**, *109*, 144801. [[CrossRef](#)] [[PubMed](#)]
30. Yumoto, H.; Mimura, H.; Koyama, T.; Matsuyama, S.; Tono, K.; Togashi, T.; Inubushi, Y.; Sato, T.; Tanaka, T.; Kimura, T.; et al. Focusing of X-ray free-electron laser pulses with reflective optics. *Nat. Photonics* **2013**, *7*, 43–47. [[CrossRef](#)]
31. Kameshima, T.; Ono, S.; Kudo, T.; Ozaki, K.; Kirihara, Y.; Kobayashi, K.; Inubushi, Y.; Yabashi, M.; Horigome, T.; Holland, A.; et al. Development of an X-ray pixel detector with multi-port charge-coupled device for X-ray free-electron laser experiments. *Rev. Sci. Instrum.* **2014**, *85*, 033110. [[CrossRef](#)] [[PubMed](#)]
32. Mimura, H.; Yumoto, H.; Matsuyama, S.; Koyama, T.; Tono, K.; Inubushi, Y.; Togashi, T.; Sato, T.; Kim, J.; Fukui, R.; et al. Generation of 1020 Wcm⁻² hard X-ray laser pulses with two-stage reflective focusing system. *Nat. Commun.* **2014**, *5*, 3539. [[CrossRef](#)] [[PubMed](#)]
33. Song, C.; Tono, K.; Park, J.; Ebisu, T.; Kim, S.; Shimada, H.; Kim, S.; Gallagher-Jones, M.; Nam, D.; Sato, T.; et al. Multiple application X-ray imaging chamber for single-shot diffraction experiments with femtosecond X-ray laser pulses. *J. Appl. Cryst.* **2014**, *47*, 188–197. [[CrossRef](#)]
34. Tono, K.; Nango, E.; Sugahara, M.; Song, C.; Park, J.; Tanaka, T.; Tanaka, R.; Joti, Y.; Kameshima, T.; Ono, S.; et al. Diverse application platform for hard X-ray diffraction in SACLA (DAPHNIS): Application to serial protein crystallography using an X-ray free-electron laser. *J. Synchrotron Rad.* **2015**, *22*, 532–537. [[CrossRef](#)] [[PubMed](#)]
35. Joti, Y.; Kameshima, T.; Yamaga, M.; Sugimoto, T.; Okada, K.; Abe, T.; Furukawa, Y.; Ohata, T.; Tanaka, R.; Hatsui, T.; et al. Data acquisition system for X-ray free-electron laser experiments at SACLA. *J. Synchrotron Rad.* **2015**, *22*, 571–576. [[CrossRef](#)] [[PubMed](#)]
36. Sato, T.; Togashi, T.; Ogawa, K.; Katayama, T.; Inubushi, Y.; Tono, K.; Yabashi, M. Highly efficient arrival timing diagnostics for femtosecond X-ray and optical laser pulses. *Appl. Phys. Exp.* **2015**, *8*, 012702. [[CrossRef](#)]
37. Katayama, T.; Owada, S.; Togashi, T.; Ogawa, K.; Karvinen, P.; Vartiainen, I.; Eronen, A.; David, C.; Sato, T.; Nakajima, K.; et al. A beam branching method for timing and spectral characterization of hard X-ray free electron lasers. *Struct. Dyn.* **2016**, *3*, 034301. [[CrossRef](#)] [[PubMed](#)]
38. Hara, T.; Inubushi, Y.; Katayama, T.; Sato, T.; Tanaka, H.; Tanaka, T.; Togashi, T.; Togawa, K.; Tono, K.; Yabashi, M.; Ishikawa, T. Two-colour hard X-ray free-electron laser with wide tenability. *Nat. Commun.* **2013**, *4*, 2919. [[CrossRef](#)] [[PubMed](#)]

39. Koyama, T.; Yumoto, H.; Miura, T.; Tono, K.; Togashi, T.; Inubushi, Y.; Katayama, T.; Kim, J.; Matsuyama, S.; Yabashi, M.; et al. Damage threshold of coating materials on X-ray mirror for X-ray free electron laser. *Rev. Sci. Instrum.* **2016**, *87*, 051801. [[CrossRef](#)] [[PubMed](#)]
40. Suzuki, M.; Inubushi, Y.; Yabashi, M.; Ishikawa, T. Polarization control of an X-ray free-electron laser with a diamond phase retarder. *J. Synchrotron Rad.* **2014**, *21*, 466–472. [[CrossRef](#)] [[PubMed](#)]
41. Tono, K.; Togashi, T.; Inubushi, Y.; Katayama, T.; Owada, S.; Yabuuchi, T.; Kon, A.; Inoue, I.; Osaka, T.; Yumoto, H.; et al. Overview of optics, photon diagnostics and experimental instruments at SACLA: Development, operation and scientific applications. *Proc. SPIE* **2017**. to be published.
42. Mafuné, F.; Miyajima, K.; Tono, K.; Takeda, Y.; Kohno, J.; Miyachi, N.; Kobayashi, J.; Joti, Y.; Nango, E.; Iwata, S.; Yabashi, M. Microcrystal delivery by pulsed liquid droplet for serial femtosecond crystallography. *Acta Cryst. D* **2016**, *72*, 520–523. [[CrossRef](#)] [[PubMed](#)]
43. David, C.; Nöhammer, B.; Ziegler, E. Wavelength tunable diffractive transmission lens for hard X rays. *Appl. Phys. Lett.* **2001**, *79*, 1088–1090. [[CrossRef](#)]
44. Gorgisyan, I.; Ischebeck, R.; Erny, C.; Dax, A.; Patthey, L.; Pradervand, C.; Sala, L.; Milne, C.; Lemke, H.T.; Hauri, C.P. THz streak camera method for synchronous arrival time measurement of two-color hard X-ray FEL pulses. *Opt. Express* **2017**, *25*, 2080–2091. [[CrossRef](#)]
45. Inoue, I.; Inubushi, Y.; Sato, T.; Tono, K.; Katayama, T.; Kameshima, T.; Ogawa, K.; Togashi, T.; Owada, S.; Amemiya, Y.; et al. Observation of femtosecond X-ray interactions with matter using an X-ray-X-ray pump-probe scheme. *Proc. Natl. Acad. Sci. USA* **2016**, *113*, 1492–1497. [[CrossRef](#)] [[PubMed](#)]
46. Osaka, T.; Yabashi, M.; Sano, Y.; Tono, K.; Inubushi, Y.; Sato, T.; Matsuyama, S.; Ishikawa, T.; Yamauchi, K. A Bragg beam splitter for hard X-ray free-electron lasers. *Opt. Express* **2013**, *21*, 2823–2831. [[CrossRef](#)] [[PubMed](#)]
47. Osaka, T.; Hirano, T.; Sano, Y.; Inubushi, Y.; Matsuyama, S.; Tono, K.; Ishikawa, T.; Yamauchi, K.; Yabashi, M. Wavelength-tunable split-and-delay optical system for hard X-ray free-electron lasers. *Opt. Express* **2016**, *24*, 9187–9201. [[CrossRef](#)] [[PubMed](#)]
48. Hirano, T.; Osaka, T.; Sano, Y.; Inubushi, Y.; Matsuyama, S.; Tono, K.; Ishikawa, T.; Yabashi, M.; Yamauchi, K. Development of speckle-free channel-cut crystal optics using plasma chemical vaporization machining for coherent X-ray applications. *Rev. Sci. Instrum.* **2016**, *87*, 063118. [[CrossRef](#)] [[PubMed](#)]



© 2017 by the authors. Licensee MDPI, Basel, Switzerland. This article is an open access article distributed under the terms and conditions of the Creative Commons Attribution (CC BY) license (<http://creativecommons.org/licenses/by/4.0/>).